JOC Article

Design, Synthesis, and Properties of Conformationally Fixed Semiquinone Monoradical Species

David A. Shultz,[†] Joseph C. Sloop,*[,‡] and Gary Washington[‡]

Department of Chemistry, North Carolina State University, P.O. Box 8204, Raleigh, North Carolina 27695, and Department of Chemistry and Life Science, United States Military Academy, 646 Swift Road, West Point, New York 10996

joseph.sloop@usma.edu

Received July 19, 2006

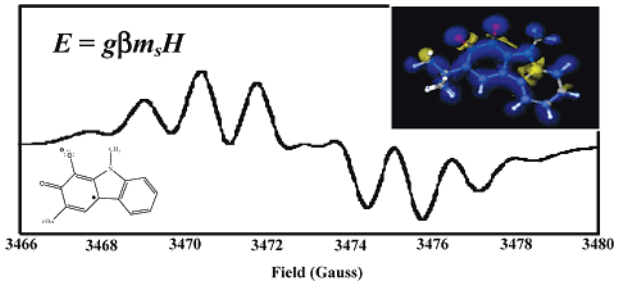

The design of novel, functionalized semiquinone (SQ) ligands which combine structural rigidity and electron-withdrawing, electron-donating, and electroneutral substituents enables investigation of multiple structure−property relationships and building blocks for new materials, including components of sensors, switches, and molecular spintronics. Along these lines, we report the synthesis of several new SQ ligands containing fused heterocyclic ring systems. Using both electron paramagnetic resonance spectroscopy and quantum chemical calculations, we show how spin density is affected by the fused ring system substituents.

Introduction

New paramagnetic ligands are of general interest in both organic and inorganic chemistry as components of sensors, switches, and molecular spintronics.[1−8] Previous research in our group has shown that both conformation and substituents can modulate spin density and exchange coupling in radical and biradical ligands.[9−11] The design of novel, functionalized semiquinone (SQ) ligands which combine structural rigidity and electron-withdrawing, electron-donating, and electroneutral substituents enables investigation of multiple structure−property relationships and building blocks for new materials. Along these lines, we report the synthesis of new SQ ligands shown in Scheme 1.

To acquire these new ligand species, the retrosynthetic strategy shown in Scheme 1 was employed.

Schemes 2−5 describe the preparation of fused, tricyclic semiquinone precursors. These compounds add both carbocyclic and heterocyclic, conformationally "locked" species to allow expansion of our investigation of substituent effects on exchange coupling between SQ moieties[9] to include substituted SQ−paramagnetic metal ion exchange coupled species.

* To whom correspondence should be addressed. Tel: (845) 938-3904.
[†] North Carolina State University.
[‡]United States Military Academy.

(1) Wolf, S. A.; Awschalom, D. D.; Buhrman, R. A.; Daughton, J. M.; von Molnar, S.; Roukes, M. L.; Chtchelkanova, A. Y.; Treger, D. M. *Science* **2001**, *294*, 1488−1495.
(2) Moser, J.-E. *Nat. Mater.* **2005**, *4*, 723−724.
(3) Tagami, K.; Tsukada, M. *J. Phys. Chem. B* **2004**, *108*, 6441−6444.
(4) Yuasa, J.; Suenobu, T.; Fukuzumi, S. *J. Phys. Chem. A* **2005**, *109*, 9356−9362.
(5) Suenaga, Y.; Pierpont, C. G. *Inorg. Chem.* **2005**, *44*, 6183−6191.
(6) Evangelio, E.; Ruiz-Molina, D. *Eur. J. Inorg. Chem.* **2005**, 2957−2971.
(7) Sato, O. *J. Photochem. Photobiol. C: Photochem. Rev.* **2004**, *5*, 203−223.
(8) Dei, A.; Gatteschi, D.; Sangregorio, C.; Sorace, L. *Acc. Chem. Res.* **2004**, *37*, 827−835.
(9) Shultz, D. A.; Bodnar, S. H.; Lee, H.; Kampf, J. W.; Incarvito, C. D.; Rheingold, A. L. *J. Am. Chem. Soc.* **2002**, *124*, 10054−10061.
(10) Shultz, D. A.; Fico, R. M., Jr.; Bodnar, S. H.; Kumar, R. K.; Vostrikova, K. E.; Kampf, J. W.; Boyle, P. D. *J. Am. Chem. Soc.* **2003**, *125*, 11761−11771.
(11) Shultz, D. A.; Fico, R. M., Jr.; Lee, H.; Kampf, J. W.; Kirschbaum, K.; Pinkerton, A. A.; Boyle, P. D. *J. Am. Chem. Soc.* **2003**, *125*, 15426−15432.

10.1021/jo061502j CCC: $33.50 © 2006 American Chemical Society
Published on Web 10/20/2006

SCHEME 1. Planar Semiquinone Retrosynthetic Strategy

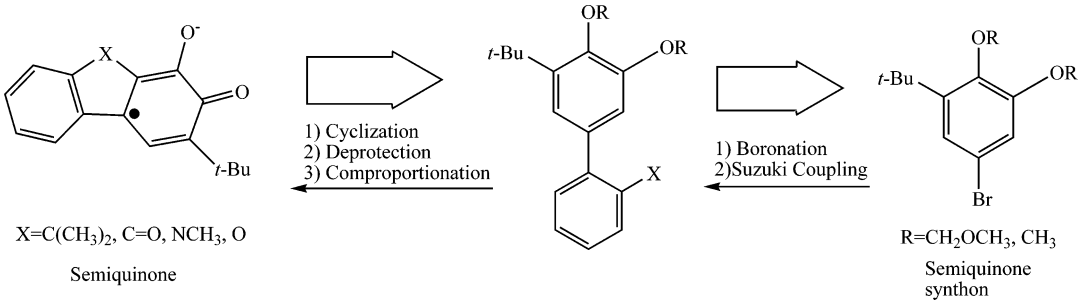

SCHEME 2. 3-*t*-Butyl-9,9-dimethylfluorene Semiquinone Synthesis[a]

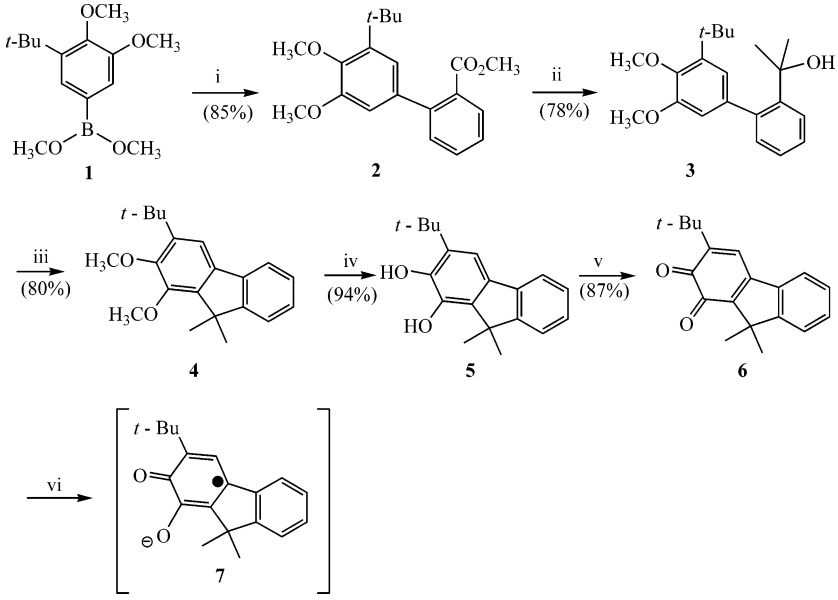

[a] Conditions: (i) Methyl 2-bromobenzoate (1 equiv), $Pd(PPh_3)_4$ (5 mol %), EtOH, Na_2CO_3, THF, reflux; (ii) (1) CH_3MgBr, THF, (2) H_30^+; (iii) PPA, 20 min; (iv) BBr_3, CH_2Cl_2, −78 °C → rt, 27 h; (v) Fétizon's reagent, Na_2SO_4, CH_2Cl_2, 24 h; (vi) **5**, KH, THF, 30 min.

Results and Discussion

Synthesis. As shown in Scheme 2, an intramolecular Friedel−Crafts-type alkylation from 2′(2-hydroxypropyl)-5-*t*-butyl-3,4-dimethoxybiphenyl (**3**) gave rise to 3-*t*-butyl-1,2-dimethoxy-9,9-dimethylfluorene (**4**).[12,13] Compound **4** was subsequently deprotected to yield catechol **5** and then oxidized to quinone **6**. Comproportionation of **5** and **6** provided SQ **7**.

An intermediate common to both Schemes 2 and 3, compound **2**, served as an intramolecular Friedel−Crafts acylating agent, yielding the fluorenone derivative **8**. However, it was found that oxidation of **9** with Fétizon's reagent[14] did not occur. The exact reason for this is unknown, but could be due, in part, to the stability of the catechol when in the keto−enol form shown in Figure 1.

Nevertheless, oxidation of the conjugate base to the SQ **10** was accomplished using ferrocenium, and the resulting EPR spectrum is consistent with SQ formation.

Attempts to prepare the *N*-protected carbazole catechol **15** from **1** ultimately resulted in partial deprotection of the amine during treatment of compound A with BBr_3, yielding a large proportion of compound B (Figure 2).

A second synthesis from **11** avoided this pitfall, as the conditions for deprotection of the MOM groups are much less vigorous. Cyclization[15] of 5-*t*-butyl-2′-nitro-2,3-dimethoxymethylenoxybiphenyl (**12**) to the regioisomeric 4-*t*-butyl-2,3-dimethoxymethylenoxycarbazole (**13a**) and 2-*t*-butyl-3,4-dimethoxymethylenoxycarbazole (**13b**) found in Scheme 4 likely occurs via a nitrenoid species and does not result in premature hydrolysis of the methoxymethyl protecting groups. The major isomer, **13a**, was that anticipated based on cyclization away from the bulky *tert*-butyl group. Although protection of the carbazole amine moiety in compounds **13a** and **13b** was successful, deprotection of the methylated carbazole derived from **13b** led to an unstable catechol which decomposed before it could be characterized. For this reason, the remaining synthetic steps from **13a** were employed. Only the stable catechol, **15**, was subsequently oxidized to the quinone, **16**. The SQ **17** was prepared via comproportionation of **15** and **16**.

(12) Shultz, D. A.; Lee, H.; Fico, R. M., Jr. *Tetrahedron* **1999**, *55*, 12079−12086.
(13) Shultz, D. A.; Boal, A. K.; Lee, H.; Farmer, G. T. *J. Org. Chem.* **1999**, *64*, 4386−4396.
(14) Balogh, V.; Fétizon, M.; Golfier, M. *J. Org. Chem.* **1971**, *36*, 1339−1341.
(15) Zim, D.; Lando, V. R.; Dupont, J.; Monteiro, A. L. *Org. Lett.* **2001**, *3*, 3049−3051.

SCHEME 3. 3-*t*-Butyl-9-fluorenone Semiquinone Synthesis[a]

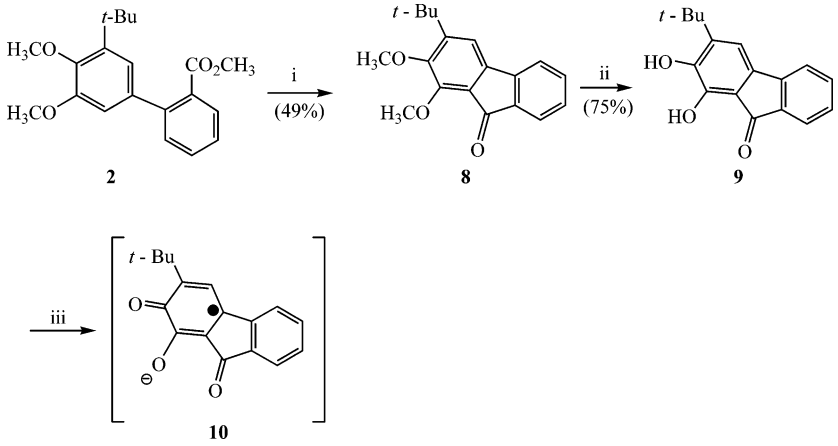

[a] Conditions: (i) PPA, 20 min; (ii) BBr_3, CH_2Cl_2, −78 °C → rt, 24 h; (iii) KH, ferrocenium (0.74 equiv), THF, 0.3 h.

SCHEME 4. 3-*t*-Butyl-9-*N*-methylcarbazole Semiquinone Synthesis[a]

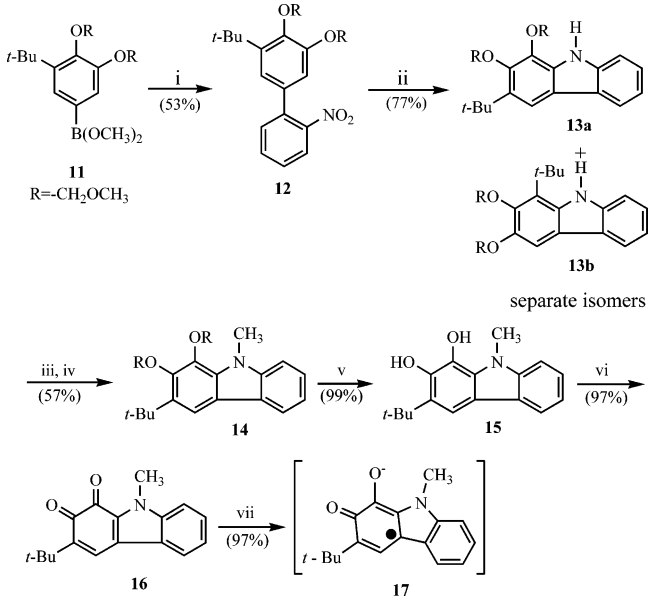

[a] Conditions: (i) 1-Bromo-2-nitrobenzene (1 equiv), $Pd(PPh_3)_4$ (5 mol %), EtOH, Na_2CO_3, THF, reflux; (ii) $P(OC_2H_5)_3$, 108 °C, 96 h; (iii) NaH, DMF; (iv) CH_3I, 60 °C, 2 h; (v) CH_3OH, reflux, 24 h; (vi) Fétizon's reagent, Na_2SO_4, CH_2Cl_2, 24 h; (vii) **15**, KH, THF, 30 min.

The dibenzofuran (Scheme 5) preparation took advantage of the ability to oxidize dibenzofuran-1-boronic acid, **18**, and 1-methoxydibenzofuran, **20**, both of which subsequently rearrange in a fashion reminiscent of the hydroboration−oxidation of alkenes to alcohols, providing the phenolic compounds **19** and **21**. It was necessary to protect the phenol **21** prior to formation of compound **23** since O-alkylation of **21** occurred to the exclusion of C-alkylation during the butylation step in route to dibenzofuran **23**. Assignments of the *tert*-butyl group position in **23a** and **23b** were made by ^1H NMR chemical shifts and coupling constants, as well as ^{13}C chemical shifts. Deprotection to the catechols **24a** and **24b** was effected without incident, but normal oxidative conditions with Fétizon's reagent failed to produce the quinones. Nonetheless, oxidation of the conjugate bases using ferrocenium provided the semiquinones **25a** and **25b**, permitting EPR spectra to be recorded.

Quinone−Semiquinone Cyclic Voltammetry. As indicated earlier, oxidation of the catechols with Fétizon's reagent gave the quinones in two cases, **6** and **16**. Cyclic voltammetric (CV) measurements for the quinone−SQ redox couple were performed as described previously,[16] and the reduction potentials relative to ferrocene are listed in Table 1.

Typical quinone−SQ redox potentials are ∼ −0.6 to ∼ −0.85 V.[17,18] As shown, the planar quinone−SQ redox potentials are more negative than similar meta- or para-substituted quinones bearing alkyl groups which are not conformationally constrained.[12,18] The planar quinones have functional groups attached directly to the quinone ring and can therefore donate electron density effectively into the ring, either inductively (in the case of **6**) or mesomerically (in the case of **16**), thereby moving the reduction to more negative potentials by ca. 250 mV. This is a rather large shift in reduction potential,[10,19] which suggests a strong substituent effect on LUMO energy.

Semiquinone Spin Density Calculations and EPR Spectroscopy. Substituents have been shown to alter spin density distribution in a wide variety of organic radicals.[20−27] Since it is our ultimate goal to explore substituent effects on exchange

(16) Shultz, D. A.; Farmer, G. T. *J. Org. Chem.* **1998**, *63*, 6254−6257.
(17) Stallings, M. D.; Morrison, M. M.; Sawyer, D. T. *Inorg. Chem.* **1981**, *20*, 2655−2660.
(18) Shultz, D. A.; Boal, A. K.; Lee, H.; Farmer, G. T. *J. Org. Chem.* **1998**, *63*, 9462−9469.
(19) Shultz, D. A.; Vostrikova, K. E.; Bodnar, S. H.; Koo, H. J.; Whangbo, M. H.; Kirk, M. L.; Depperman, E. C.; Kampf, J. W. *J. Am. Chem. Soc.* **2003**, *125*, 1607−1617.
(20) Neugebauer, F. A.; Fischer, P. H. H. *Z. Naturforsch.* **1966**, *21b*, 1036.
(21) Strom, E. T.; Bluhm, A. L.; Weinstein, J. *J. Org. Chem.* **1967**, *32*, 3853−3856.
(22) Church, D. F. *J. Org. Chem.* **1986**, *51*, 1138−1140.
(23) Zhang, Y. H.; Jiang, B.; Zhou, C. M.; Jiang, X. K. *Chin. J. Chem.* **1994**, *12*, 516−523.
(24) Miura, Y.; Kitagishi, Y.; Ueno, S. *Bull. Chem. Soc. Jpn* **1994**, *67*, 3282−3288.
(25) Jackson, R. A.; Sharifi, M. *J. Chem. Soc., Perkin Trans. 2* **1996**, 775−778.
(26) Boesch, S. E.; Wheeler, R. A. *J. Phys. Chem. A* **1997**, *101*, 8351−8359.
(27) Shultz, D. A.; Gwaltney, K. P.; Lee, H. *J. Org. Chem.* **1998**, *63*, 769−774.

SCHEME 5. Dibenzofuran Semiquinone Synthesis[a]

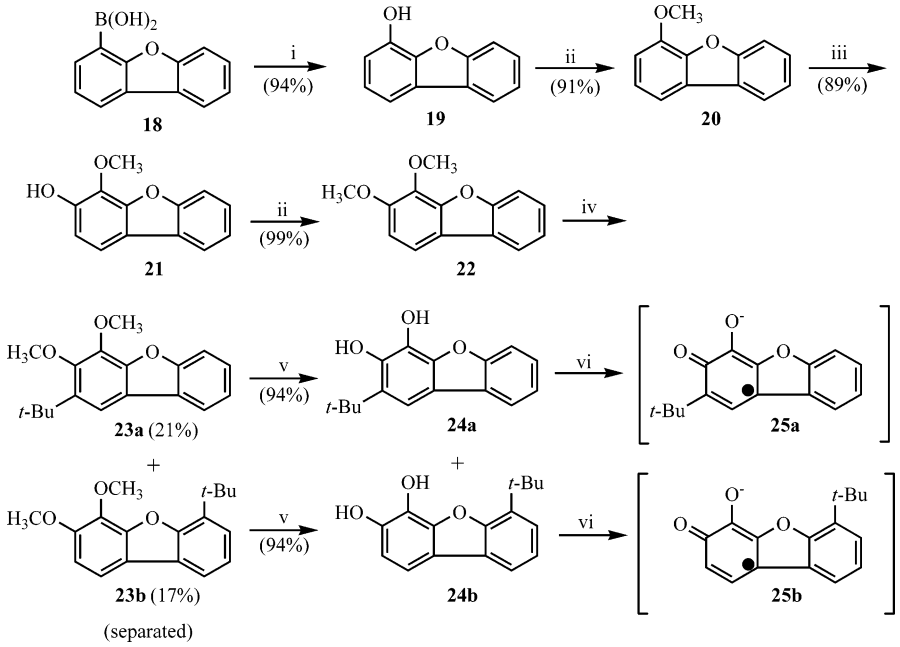

[a] Conditions: (i) H_2O_2, NaOH, 24 h; (ii) (1) K_2CO_3, 18-crown-6 (2 mol %), (2) CH_3I; (iii) (1) *t*-BuLi, THF, −78 °C, (2) $B(OCH_3)_3$, rt, 24 h, (3) H_2O_2, NaOH, 24 h; (iv) *t*-BuOH, PPA, H_3PO_4, 76 °C, 24 h; (v) BBr_3, CH_2Cl_2, −78 °C → rt, 24 h; (vi) KH, ferrocenium (0.74 equiv), THF, 0.3 h.

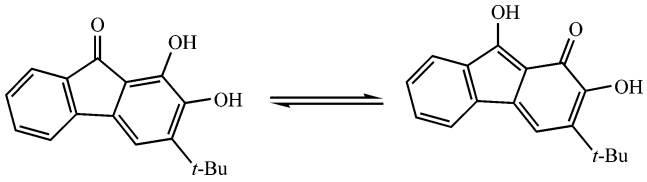

FIGURE 1. Fluorenone catechol keto−enol equilibrium.

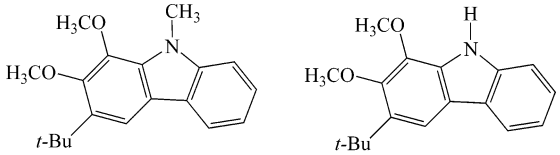

Compound A Compound B

FIGURE 2. Carbazole N-deprotection.

coupling of our SQ ligands with paramagnetic metal ions, it is desirable to evaluate spin density distribution in our new SQ ligands. Theoretical spin density distribution contours for the semiquinones without solvent (gas phase) generated from Gaussian 98W density functional computations with full geometry optimization employing an unrestricted B3LYP method and the epr-ii basis set[28] predict substituent modulation of spin density in compounds **7**, **10**, **17**, **25a**, and **25b** (see Figure 3). Proton hyperfine coupling constants (absolute values) obtained via computation are provided in Table 2.

TABLE 1. Planar Quinone−Semiquinone Reduction Potentials[a]

redox couple	potential (V)
6⇌**7**	−0.94
16⇌**17**	−0.97

[a] Cyclic voltammograms are available in Supporting Information.

As shown in Figure 3, while a majority of the spin density is retained in the SQ ring for these systems, it is apparent that substituents also affect the distribution of phenyl ring spin density. Theoretical hyperfine coupling constants reported in Table 2 provide some quantitative evidence of the extent of this spin density modulation.

To further evaluate spin density distributions in our planar SQ solution phase, X-band EPR spectra were collected for each SQ in THF solvent at room temperature. The spectra and simulations[30] are shown in Figure 4, and the a_H values are listed in Table 2. To facilitate the discussion of our data, SQ ligands are listed in Table 2 in order of decreasing electron donation from left to right.

A comparison of the EPR spectra recorded in Figure 4 and experimental a_H values found in Table 2 reveals some similarities with those of SQs in previously reported work. In terms of general appearance, the spectra are well resolved except for SQs **10** and **17**, where line broadening and obscuration of the hyperfine coupling constants may result from spin exchange due to higher EPR solution concentration and species instabil-

(28) Spin densities and a_H values determined by Gaussian 98 for the semiquinones without solvent (gas phase): Frisch, M. J.; Trucks, G. W.; Schlegel, H. B.; Scuseria, G. E.; Robb, M. A.; Cheeseman, J. R.; Zakrzewski, V. G.; Montgomery, J. A., Jr.; Stratmann, R. E.; Burant, J. C.; Dapprich, S.; Millam, J. M.; Daniels, A. D.; Kudin, K. N.; Strain, M. C.; Farkas, O.; Tomasi, J.; Barone, V.; Cossi, M.; Cammi, R.; Mennucci, B.; Pomelli, C.; Adamo, C.; Clifford, S.; Ochterski, J.; Petersson, G. A.; Ayala, P. Y.; Cui, Q.; Morokuma, K.; Malick, D. K.; Rabuck, A. D.; Raghavachari, K.; Foresman, J. B.; Cioslowski, J.; Ortiz, J. V.; Stefanov, B. B.; Liu, G.; Liashenko, A.; Piskorz, P.; Komaromi, I.; Gomperts, R.; Martin, R. L.; Fox, D. J.; Keith, T.; Al-Laham, M. A.; Peng, C. Y.; Nanayakkara, A.; Gonzalez, C.; Challacombe, M.; Gill, P. M. W.; Johnson, B. G.; Chen, W.; Wong, M. W.; Andres, J. L.; Head-Gordon, M.; Replogle, E. S.; Pople, J. A. *Gaussian 98*, revision A.9; Gaussian, Inc.: Pittsburgh, PA, 1998.

(29) Spin density contours obtained using the GNU Image Manipulation Program, 1991. For more information, see www.gimp.org.

(30) Duling, D. *EPR Calculations for MS-Windows*, NT/95 Software Tools, version 0.96 ed.; Public EPR Software Tools; National Institute of Environmental Health Sciences, National Institutes of Health: Triangle Park, NC, 1996.

TABLE 2. Planar Semiquinone a_H Values[a]

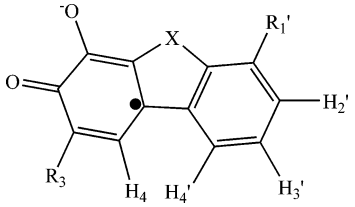

Compound	**17** X = NCH_3 R_3 = *t*-Bu R1′ = H		**25a** X = O R_3 = *t*-Bu R1′ = H		**25b** X = O R_3 = H R1′ = *t*-Bu		**7** X = $C(CH_3)_2$ R_3 = *t*-Bu R1′ = H		**10** X = C = O R_3 = *t*-Bu R1′ = H	
proton	exp[b,c]	theor[d]	exp[e]	theor[d]	exp[e]	theor[d]	exp[f]	theor[d]	exp[c,g]	theor[d]
H4	2.71	2.86	2.66	2.73	2.86	2.65	2.66	2.19	0.83	0.15
H4′	1.38	0.52	0.74	0.56	0.42	0.51	0.76	0.64	0.84	0.96
H3′	0.36	0.16	0.02	0.04	0.09	0.03	0.26	0.30	0.83	0.36
R3					0.72	1.86				
H2′	1.18	0.26	0.45	0.41	0.31	0.38	0.86	0.83	2.50	1.37
R1′	2.03	0.53	0.34	0.26			0.26	0.26	0.83	0.54
N	1.33	0.92								
$\sum a_{H'}$ (SQ ring)	2.71	2.86	2.66	2.73	3.58	4.51	2.66	2.19	0.83	0.15
$\sum a_{H'}$ (Ph ring)	4.97	1.47	1.55	1.27	0.82	0.92	2.14	2.03	5.00	3.23

[a] The a_H values in Gauss. [b] Conditions: 0.5 mM SQ in THF, 298 K, X-band frequency = 9.59 GHz. [c] EPR simulation line width (set ~1 G to obtain satisfactory spectral simulation) may limit the accuracy of experimental a_H values; see ref 31. [d] From ref 28, gas phase. [e] Conditions: catecholate oxidation with ferrocenium, 0.1 mM SQ in THF, 298 K, X-band frequency = 9.59 GHz. [f] Conditions: 0.1 mM SQ in THF, 298 K, X-band frequency = 9.77 GHz. [g] Conditions: catecholate oxidation with ferrocenium, 0.5 mM SQ in THF, 298 K, X-band frequency = 9.59GHz.

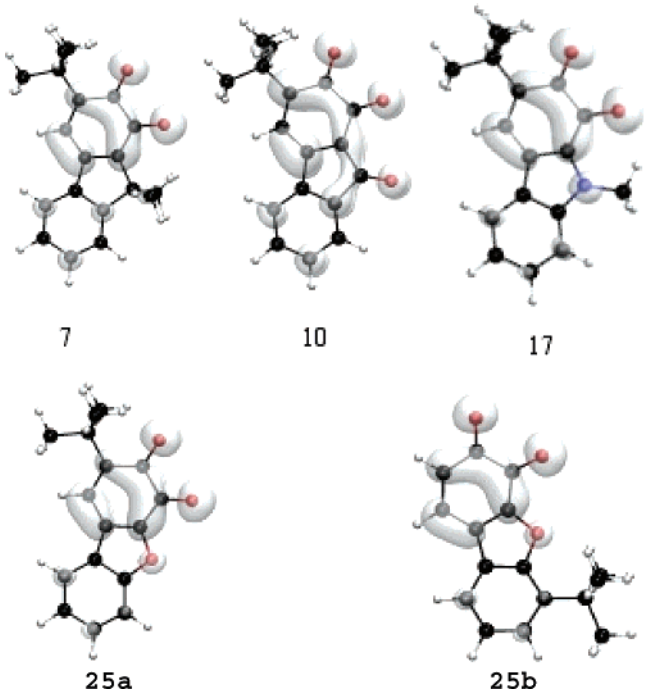

FIGURE 3. The 0.001 e/au^3 planar SQ spin density distribution contours.[29]

ity.[31,32] With the exception of SQ **10**, the largest proton hyperfine coupling constant is H_4, adjacent to the radical center.[10]

At the bottom of Table 2 are summations of SQ ring proton hyperfine coupling constants ($\sum a_H$(SQ ring)) and phenyl ring proton hyperfine coupling constants ($\sum a_H$(Ph ring)). These parameters are proportional to the spin densities in each ring according to the McConnell relationship (in which $a_H \sim \rho_C$, where ρ_C is the carbon spin density)[33] and are important in forming hypotheses regarding exchange coupling of our SQ ligands to paramagnetic metal ions and regarding exchange coupling of future SQ ligands that have stable radicals bound to the phenyl ring.

While experimental $\sum a_H$ parameters suggest that the strong electron-donating substituent (X = NCH_3) increases phenyl ring spin density relative to SQ ring spin density, the theoretical spin density contour and ab initio $\sum a_H$ results indicate a majority of the excess spin density in the SQ ring. One possibility for this discrepancy may be the large simulation line width (~1 G) required for a satisfactory fit of the spectrum, resulting in significant error associated with the smaller experimental a_H values for SQ **17**. On the basis of the theoretical results, we hypothesize that **17** will exhibit stronger exchange coupling with paramagnetic metal ions (J_{M-SQ}) provided that the major contribution to exchange is directly related to the product of spin densities on the SQ and the metal ion. Since the spin density is the square of the SOMO wavefunction, and the product of the spin densities is proportional to the overlap integral of the natural orbitals and therefore to J, see[34]

$$J_{M-SQ} \sim \rho_M \times \rho_{SQ}$$

By the same token, if stable radicals are attached to the phenyl ring of **17**, the exchange coupling between SQ and a radical ($J_{SQ-radical}$) will be smaller for **17** than for the other derivatives.

Experimental $\sum a_H$ values for the furan semiquinones **25a** and **25b** are consistent with both theoretically predicted spin density distributions and a_H values. Our results show that oxygen in

(31) Peric, M.; Bales, B. L. *J. Magn. Reson.* **2004**, *169*, 27−29.

(32) SQs **10** and **17** began showing signs of degradation within 15 min upon removal from an argon environment. This instability is of little concern since we are ultimately interested in transition metal complexes of these SQs which are, in most cases, inert.

(33) McConnell, H. M.; Chestnut, D. B. *J. Chem. Phys.* **1958**, *28*, 107−117.

(34) Kahn, O. *Molecular Magnetism*; VCH: New York, 1993.

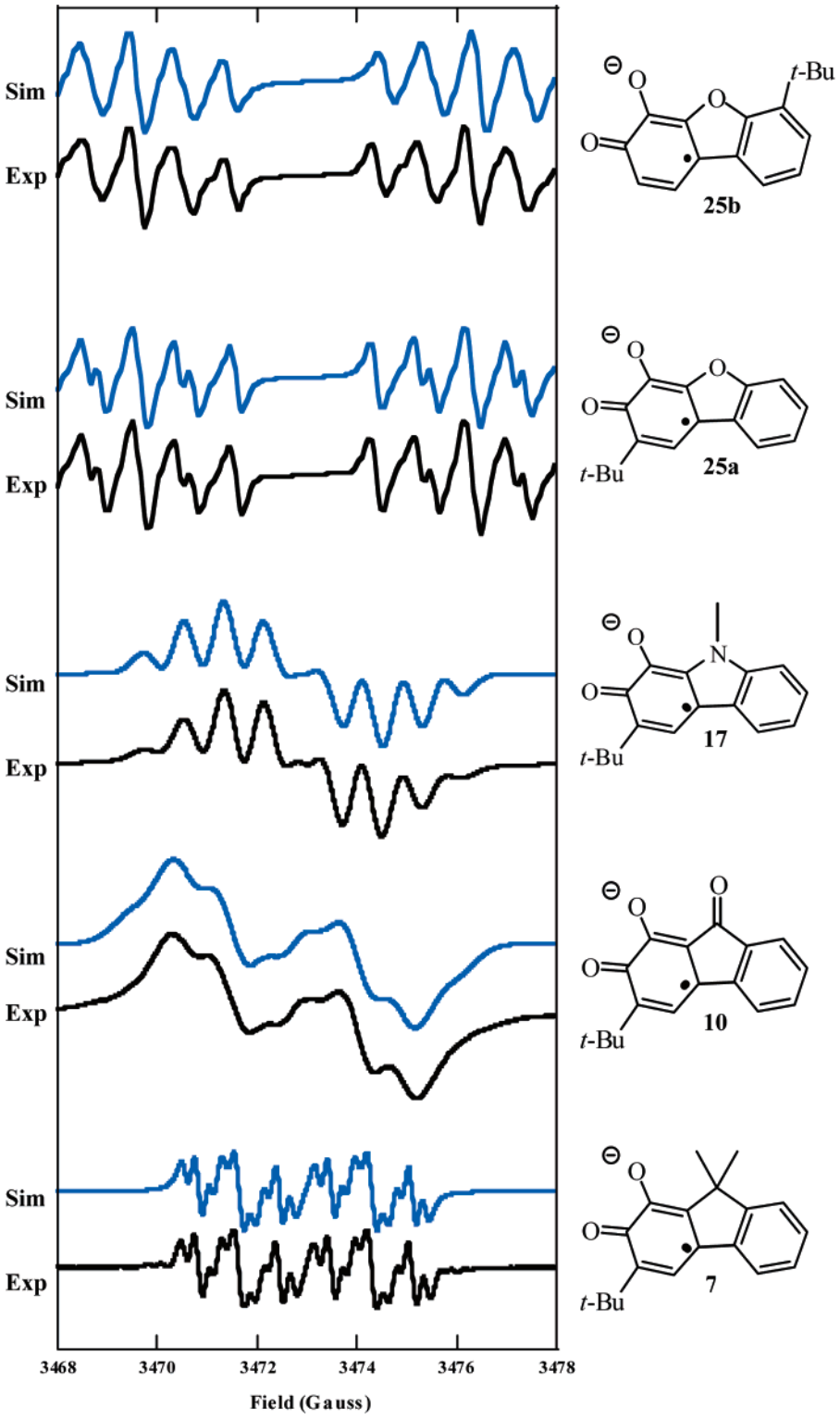

FIGURE 4. Planar SQ X-band EPR and simulations.

the heterocyclic ring systems increases spin density in the SQ ring relative to compound **7**. This is most likely due to mesomeric electron donation by the furan oxygens. Conversely, inductive electron-withdrawing properties, as evidenced by the presence of spin density on the furan oxygens, may be responsible for the decrease in spin density seen in the phenyl ring relative to that of compound **7**. Differences in the magnitudes of the SQ and phenyl ring $\sum a_H$ values in **25a** and **25b** may be accounted for by the *tert*-butyl group location.

Experimental a_H values for dimethyl fluorene SQ **7** are in agreement with theoretically derived values recorded in Table 2 and consistent with spin densities in Figure 3. As expected, the spin density is more equally distributed between the SQ

and Ph rings in SQ **7** than in the remaining planar semiquinones, a consequence of the slight inductive electron-donating nature of the $-C(CH_3)_2$ group.

Semiquinone **10** departs from the general trend described above. As in the case of **17**, the EPR spectrum was poorly resolved, potentially resulting in uncertainty in the smaller a_H values. Figure 3 clearly predicts significant resonance interaction between the carbonyl moiety, a strong electron-withdrawing substituent, and the catecholate oxygen in the semiquinone ring of **10**. The trend indicated in the theoretical and experimental $\sum a_H$ magnitudes supports this, illustrating two important results—redistribution of spin density away from the SQ ring relative to compound **7** and a concomitant increase in phenyl ring spin density. We hypothesize that **10** will exhibit weaker exchange coupling with paramagnetic metal ions (J_{M-SQ}), and by the same token, if stable radicals are attached to the phenyl ring of **10**, the exchange coupling between SQ and a radical ($J_{SQ-radical}$) will be greater for **10** than for the other derivatives.

Conclusions

Planar semiquinone species with electroneutral, electron-withdrawing, and electron-donating substituents affect hyperfine coupling constants. General trends are evident. The semiquinone hyperfine coupling constants are consistent with those previously reported. Electroneutral groups, such as $-C(CH_3)_2$ in SQ **7**, provide for a more uniform distribution of excess spin density throughout the SQ system. Electron-withdrawing groups were found to dramatically alter spin density in the planar SQ system relative to SQ **7** as evidenced by a reduction in the magnitude of the hydrogen hyperfine coupling in the SQ ring and an increase in the magnitude of SQ phenyl ring a_H values. Electron-donating groups were generally found to decrease the magnitude of the phenyl ring a_H values. Ab initio methods support these results, predicting substituent-based variations in modulation of spin density distribution in conformationally fixed semiquinone systems. Notwithstanding SQ **10** and SQ **17**, theoretically calculated a_H values were found to give good agreement with experimental hyperfine coupling constants in most cases. Our results suggest a design criterion for enhancing paramagnetic metal ion exchange coupling. Since electron-withdrawing groups increase spin density, the exchange coupling between the SQ and metal ions should be greater for SQs with electron-withdrawing groups than for SQs with electron-donating groups. We will report our findings along these lines in the future.

Experimental Section

Instrumentation. NMR data were collected at 300.0 MHz for ^{1}H and 75.4 MHz for ^{13}C. All ^{1}H and ^{13}C NMR chemical shifts reported are referenced to deuteriochloroform using the appropriate chemical shifts unless specifically noted. Reported melting points are uncorrected. X-band EPR spectra were collected at 9.59−9.77 GHz. Computations were performed on a computer platform operating at 2.8 GHz, using Gaussian 98W revision A.9.

Chemicals. Methyl-2-bromobenzoate, *o*-bromonitrobenzene, $P(OC_2H_5)_3$, and dibenzofuran-1-boronic acid (**18**) are commercially available and were used without further purification. Compounds **1** and **11** were prepared according to literature methods.[15] All reactions, solvent distillations, and EPR sample preparation were conducted under nitrogen or argon atmosphere. THF was distilled from sodium benzophenone ketyl before use, while CH_2Cl_2 and CH_3OH were distilled from CaH_2.

Experimental Procedures: 2′-Carbomethoxy-5-*t*-butyl-3,4-dimethoxybiphenyl (2). To a 125 mL Kjeldahl flask equipped with a N_2 adapter and stir bar were added methyl-2-bromobenzoate (0.52 mL, 3.70 mmol), 3-*t*-butyl-4,5-dimethoxyphenylboronic ester (0.85 g, 3.70 mmol), $Pd(PPh_3)_4$ (0.21 g, 0.19 mmol), 30 mL of dry THF, 7.4 mL of EtOH, and 11.1 mL of 2 M Na_2CO_3. A reflux condenser was added, and the reaction mixture was purged 10 times with N_2 and refluxed for 24 h. Following filtration through celite, the solvent was removed by evaporation under reduced pressure, extracted with Et_2O, washed with saturated brine solution, concentrated, and subjected to radial chromatography (silica gel w/5−40% ether/pet ether gradient) to afford 1.03 g (85%) of colorless crystals, **2**, mp 62−65 °C. ^{1}H NMR (300 MHz, $CDCl_3$): δ 7.72 (d, J = 7.62 Hz, 1H), 7.50 (m, 1H), 7.41 (m, 2H), 6.84 (dd, J = 1.95, 8.25 Hz, 2H), 3.92 (s, 3H), 3.88 (s, 3H), 3.64 (S, 3H), 1.39 (s, 9H). ^{13}C NMR (300 MHz, $CDCl_3$): δ 165.9, 152.9, 142.9, 130.8, 130.3, 129.4, 129.2, 126.8, 119.1, 110.8, 60.3, 55.7, 52.0, 34.9, 30.4. IR (cm^{-1}): ν 1719, 1291, 1248. Anal. Calcd for $C_{20}H_{24}O_4$: C, 73.14; H, 7.36. Found: C, 72.85; H, 7.32.

2′(2-Hydroxypropyl)-5-*t*-butyl-3,4-dimethoxybiphenyl (3). To an oven-dried 125 mL Schlenk flask equipped with a stir bar and N_2 adapter were added **2** (0.55 g, 1.67 mmol) and 20 mL of distilled THF. Then, CH_3MgI (2.23 mL, 6.7 mmol) was added dropwise, a reflux condenser added, and the reaction mixture refluxed for 3 h. The reaction mixture was quenched with deionized water, filtered through celite, acidified with 1 M HCl, washed with Et_2O, and the layers were separated, and solvent was removed under reduced pressure. The crude product was chromatographed on SiO_2 (deactivated w/1% Et_3N) using 20% ether/petroleum ether, yielding 0.43 g (78%) of a yellowish−brown oil, **3**, which showed facile elimination to the alkene and was hence used without further purification. ^{1}H NMR (300 MHz, $CDCl_3$): δ 7.59 (d, J = 7.86 Hz, 1H), 7.34 (t, J = 7.2 Hz, 1H), 7.24 (m, 1H), 7.12 (d, J = 7.86 Hz, 1H), 6.85 (s, 1H), 6.79 (s, 1H), 3.92 (s, 3H), 3.83 (s, 3H), 1.74 (br s, 1H), 1.51 (s, 6H), 1.37 (s, 9H). ^{13}C NMR (300 MHz, $CDCl_3$): δ 152.8, 146.3, 142.9, 140.2, 137.8, 132.2, 127.3, 126.0, 125.7,120.2, 112.3, 74.1, 60.5, 55.8, 35.2, 32.6, 30.6. IR (cm^{-1}): ν 3436, 3048, 1237.

3-*t*-Butyl-1,2-dimethoxy-9,9-dimethylfluorene (4). To a beaker were added **3** (0.25 g, 0.76 mmol) and PPA (∼2.0 g). The reaction mixture was heated to 40 °C and stirred with a glass rod for 20 min. The resulting brown solution was quenched with ice (∼10 g), washed with saturated NaCl solution, extracted with Et_2O, dried over Na_2SO_4, and the solvent removed under reduced pressure. The crude product was chromatographed on SiO_2 (deactivated w/1% Et_3N) using 20% ether/petroleum ether, yielding 0.20 g (80%) of a colorless oil, **4**. ^{1}H NMR (300 MHz, $CDCl_3$): δ 7.64 (d, J = 6.78 Hz, 1H), 7.42 (s, 1H), 7.38 (d, J = 7.86 Hz, 1H), 7.28 (m, J = 6.42 Hz, 2H), 3.93 (s, 6H), 1.59 (s, 6H), 1.46 (s, 9H). ^{13}C NMR (300 MHz, $CDCl_3$): δ 154.2, 152.5, 151.0, 143.3, 143.2, 139.3, 134.7, 126.8, 126.5, 122.1, 119.2, 112.8, 59.8, 59.7, 47.6, 35.3, 31.7, 30.8, 25.8. IR (cm^{-1}): ν 3050, 2953, 1263. Anal. Calcd for $C_{21}H_{26}O_2$: C, 81.25; H, 8.44. Found: C, 81.04; H, 8.60.

3-*t*-Butyl-1,2-dihydroxy-9,9-dimethylfluorene (5). To a 125 mL Kjeldahl flask equipped with a N_2 adapter and stir bar were added **4** (0.29 g, 0.93 mmol), 10 mL of distilled CH_2Cl_2, and the mixture was purged three times with N_2 and cooled to −78 °C. Then, a 1.0 M solution of BBr_3 (2.7 mL, 2.70 mmol) was added dropwise slowly to the reaction mixture, which was then allowed to warm to room temperature and to stir for 10 h under N_2, protected from light. The reaction mixture was quenched with ice, washed with saturated brine, and extracted with two 10 mL portions of CH_2Cl_2. The organic layers were combined and dried over Na_2SO_4, and the solvent was evaporated to dryness to afford 0.25 g (94%) of a gray solid, **5**, mp 54−60 °C (dec). ^{1}H NMR (300 MHz, $CDCl_3$): δ 7.62 (d, J = 6.75 Hz, 1H), 7.36 (dd, J = 10.1, 1.0 Hz, 1H), 7.27 (d, J = 7.86 Hz, 2H), 7.25 (d, J = 6.42

Hz, 1H), 5.36 (s, 6H), 5.12 (s, 1H), 1.61 (s, 6H), 1.46 (s, 9H). ^{13}C NMR (300 MHz, $CDCl_3$): δ 153.4, 142.7, 141.2, 141.1, 139.7, 135.9, 132.3, 126.9, 126.2, 122.0,119.1, 110.1, 47.0, 31.0, 30.0, 25.0. IR (cm^{-1}): ν 3509. Anal. Calcd for $C_{19}H_{22}O_2$: C, 80.81; H, 7.85. Found: C, 80.43; H, 7.63.

3-*t*-Butyl-9,9-dimethylfluorene orthoquinone (6). To a 100 mL round-bottom flask equipped with a N_2 adapter and stir bar were added **5** (0.116 g, 0.41 mmol), Fétizon's reagent (3.5 g, excess), Na_2SO_4 (3.5 g, excess), and distilled CH_2Cl_2 (20 mL), and the mixture was purged three times with N_2. The reaction mixture was stirred for 18 h under N_2. Filtration through celite and concentration under reduced pressure afforded 0.10 g (87%) of a red solid (Et_2O), **6**, mp 182−184 °C. ^{1}H NMR: δ 7.68 (dd, J = 7.5, 1.8 Hz, 1H), 7.49 (t, J = 9.3 Hz, 1H), 7.46 (t, J = 8.4 Hz, 1H), 7.31 (d, J = 3.1 Hz, 1H), 7.25 (s, 1H), 1.50 (s, 6H), 1.34 (s, 9H). ^{13}C NMR: δ 182.7, 175.9, 158.1, 152.1, 149.6, 145.1, 137.2, 131.0, 127.8, 127.5, 122.9, 122.4, 49.0, 35.9, 29.6, 24.5. IR (cm^{-1}): ν 1637. HRMS (M + H) (FAB+): calcd for $C_{19}H_{21}O_3$, 281.1542; found, 281.1551.

3-*t*-Butyl-9,9-dimethylfluorene semiquinone (7). To a 20 mL vial equipped with a stir bar in an inert atmosphere were added **5** (0.049 g, 0.17 mmol), **6** (0.048 g, 0.17 mmol), and dry THF (5 mL), and the mixture was stirred for 5 min. Then, KH (2 mg, 0.50 mmol) was added and the reaction mixture stirred for 30 min. The resulting suspension was filtered to remove excess KH, the semiquinone **7** was obtained as a green solution, and a 0.1 mM solution of the semiquinone in THF was prepared for EPR studies. Electrochemical preparation of **7** was accomplished by placing **6** (0.00155 g, 0.0055 mmol) and electrolyte *n*-Bu_4NPF_6 (0.21 g, 0.55 mmol) in 5.5 mL of anhydrous THF. Cyclic voltammetric measurements were then conducted on the solution, with Pt wire serving as the working and auxiliary electrodes, while the reference electrode was $Ag/AgNO_3$ in acetonitrile.

3-*t*-Butyl-1,2-dimethoxy-9-fluorenone (8). Using the procedure for **4**, this compound was obtained from **2** in 49% yield as a yellow oil, **8**. ^{1}H NMR (300 MHz, $CDCl_3$): δ 7.60 (t, J = 7.5, 0.9 Hz, 1H), 7.45 (t, J = 1.0 Hz, 1H), 7.44 (dq, J = 5.7, 0.9 Hz, 1H), 7.23 (dd, J = 6.6, 1.8 Hz, 1H), 7.20 (s, 1H), 4.09 (s, 3H), 3.93 (s, 3H), 1.41 (s, 9H). ^{13}C NMR (300 MHz, $CDCl_3$): δ 191.5, 153.6, 153.1, 150.6, 144.1, 139.5, 134.9, 134.2, 128.2, 124.0, 123.5, 119.4, 113.7, 61.9, 61.0, 35.9, 30.3. IR (cm^{-1}): ν 1707. HRMS (FAB+): calcd for $C_{19}H_{20}O_3$, 296.1412; found, 296.1407.

3-*t*-Butyl-1,2-dihydroxy-9-fluorenone (9). Using method B described in the Supporting Information, this compound was obtained in 75% yield as a red solid (Et_2O), **9**, mp 144−146 °C (dec). ^{1}H NMR (300 MHz, $CDCl_3$): δ 8.07 (br s, 1H), 7.56 (d, J = 7.08 Hz, 1H), 7.42 (d, J = 2.46 Hz, 2H), 7.18 (q, J = 3.66 Hz, 1H), 6.99 (s, 1H), 5.74 (s, 1H), 1.44 (s, 9H). ^{13}C NMR (300 MHz, $CDCl_3$): δ 194.8, 176.3, 151.3, 148.3, 146.5, 136.9, 134.8, 133.7, 132.0, 126.1, 124.1, 112.9, 110.3, 34.2, 28.9. IR (cm^{-1}): ν 3503, 3389, 1684. HRMS (M + H) (FAB+): calcd for $C_{17}H_{17}O_3$, 269.1178; found, 269.1174.

3-*t*-Butyl-9-fluorenone semiquinone (10). To a 20 mL vial in an inert atmosphere were added **9** (0.0082 g, 0.03 mmol, 0.250 mmol), ferrocenium (0.0061 g, 0.022 mmol), 2 mL of degassed THF, and KH (∼1 mg). The solution was stirred for 20 min. The resulting green suspension was filtered to remove excess KH, and a 0.1 mM solution of the semiquinone in THF was prepared for EPR studies.

5-*t* -Butyl-2′-nitro-2,3-dimethoxymethylenoxybiphenyl (12). To a 125 mL Kjeldahl flask equipped with a N_2 adapter and stir bar were added 2-bromonitrobenzene (0.40 g, 1.98 mmol), 3-*t*-butyl-4,5-dimethoxymethylenephenylboronic ester (1.23 g, 3.77 mmol), $Pd(PPh_3)_4$ (0.20 g, 0.18 mmol), dry THF (50 mL), EtOH (7.5 mL), and 2 M Na_2CO_3 (11.3 mL). A reflux condenser was added, and the reaction mixture was purged 10 times with N_2 and refluxed for 24 h. Following filtration through celite, the solvent was removed by evaporation under reduced pressure, extracted with Et_2O, washed with saturated brine solution, concentrated, and subjected to radial chromatography (silica gel w/0−30% ether/pet ether gradient) to afford 0.39 g (53%) of a yellow oil, **12**. ^{1}H NMR (300 MHz, $CDCl_3$): δ 7.78 (d, J = 8.04 Hz, 1H), 7.58 (t, J = 7.2 Hz, 1H), 7.46 (d, J = 7.7 Hz, 2H), 7.02 (d, J = 1.4 Hz, 1H), 6.94 (d, J = 1.47 Hz, 1H), 5.26 (s, 2H), 5.18 (s, 2H), 3.57 (s, 3H), 3.51 (s, 3H), 1.42 (s, 9H). ^{13}C NMR: δ 150.2, 146.1, 143.7, 135.8, 132.6, 131.3, 131.2, 128.6, 127.2, 119.4, 115.4, 114.7, 99.1, 95.6, 57.5, 56.7, 35.4, 30.2. IR (cm^{-1}): ν 1525. HRMS (FAB+): calcd for $C_{20}H_{25}NO_6$, 375.1682; found, 375.1668.

4-*t*-Butyl-2,3-dimethoxymethylenoxycarbazole (13a) and 2-*t*-Butyl-3,4-dimethoxymethylenoxycarbazole (13b). To a 25 mL round-bottom flask equipped with a N_2 adapter and stir bar were added **12** (0.27 g, 0.86 mmol) and $P(OC_2H_5)_3$ (1.5 mL, 8.75 mmol). The reaction mixture was purged three times with N_2 and refluxed at 108 °C for 96 h under N_2. Filtration through celite, removal of solvent by vacuum distillation, and radial chromatography (silica gel w/0−50% ether/pet ether gradient) afforded the colorless oils **13a** (0.18 g) and **13b** (0.060 g) (conversion rate of 81%). **13a:** ^{1}H NMR ($CDCl_3$, 300 MHz): δ 8.41 (br s, 1H), 7.97 (d, J = 7.80 Hz, 1H), 7.74 (s, 1H), 7.39 (s, 1H), 7.36 (q, J = 7.50 Hz, 1H), 7.19 (t, J = 7.00 Hz, 1H), 5.28 (s, 2H), 5.25 (s, 2H), 3.68 (s, 3H), 3.60 (s, 3H), 1.76 (s, 9H). ^{13}C NMR: δ 145.5, 139.4, 133.7, 125.7, 124.5, 122.6, 119.8, 110.0, 105.6, 98.6, 58.5, 55.5, 37.1, 32.4. IR (cm^{-1}): ν 3503. HRMS (FAB+): calcd for $C_{20}H_{25}NO_4$, 343.1784; found, 343.1781. **13b:** ^{1}H NMR ($CDCl_3$, 300 MHz): δ 9.07 (s, 1H), 7.99 (d, J = 7.80 Hz, 1H), 7.76 (s, 1H), 7.41 (t, J = 8.04 Hz, 1H), 7.36 (t, J = 7.02 Hz, 1H), 7.19 (t, J = 7.29 Hz, 1H), 5.29 (s, 2H), 5.26 (s, 2H), 3.73 (s, 3H), 3.69 (s, 3H), 1.52 (s, 9H). ^{13}C NMR: δ 146.8, 139.7, 135.5, 131.1, 125.8, 120.5, 120.1, 112.3, 99.6, 98.6, 58.2, 58.1, 35.3, 31.0. IR (cm^{-1}): ν 3365. HRMS (FAB+): calcd for $C_{20}H_{25}NO_4$, 343.1784; found, 343.1772.

9*N*-Methyl-4-*t*-butyl-2,3-dimethoxymethylenoxycarbazole (14). To a 100 mL round-bottom flask equipped with a stir bar were added **13a** (0.292 g, 0.85 mmol) and 4 mL of dry DMF, and the mixture was heated to 60 °C under N_2. To this was added a suspension of NaH (0.044 g, 1.85 mmol) in 6.1 mL of dry DMF (heated at 60 °C). The reaction mixture was stirred for 1 h under N_2. Then, CH_3I (0.12 mL, 1.85 mmol) was added dropwise slowly via syringe and stirred for an additional 1 h. Removal of solvent by vacuum distillation and chromatography (silica gel w/0−10% ether/pet ether gradient) afforded 0.172 g (57%) (conversion rate of 82%) of a pale yellow oil, **14**. ^{1}H NMR ($CDCl_3$, 300 MHz): δ 7.93 (d, J = 7.62 Hz, 1H), 7.68 (s, 1H), 7.40 (q, J = 6.9 Hz, 1H), 7.37 (t, J = 7.8 Hz, 1H), 7.21 (t, J = 7.26 Hz, 1H), 5.30 (s, 2H), 5.13 (s, 2H), 3.79 (s, 3H), 3.68 (s, 3H), 3.60 (s, 3H), 1.74 (s, 9H). ^{13}C NMR: δ 147.4, 146.1, 140.0, 130.5, 126.2, 124.9, 122.5, 120.6, 111.9, 105.2, 100.6, 96.3, 95.6, 81.9, 57.2, 55.9, 41.6, 36.3, 33.6. IR (cm^{-1}): ν 1472, 1381. HRMS (FAB+): calcd for $C_{21}H_{27}NO_4$, 357.1940; found, 357.1926.

9*N*-Methyl-4-*t*-butyl-2,3-dihydroxycarbazole (15). To a 100 mL round-bottom flask equipped with a stir bar were added **14** (0.16 g, 0.45 mmol), 1 mL of concentrated HCl, and 40 mL of methanol. A reflux condenser was attached, and the mixture was refluxed for 24 h with stirring under N_2, protected from light. The solvent was removed by evaporation under reduced pressure. The residue was taken up in CH_2Cl_2, extracted with saturated brine, and the organic layer dried over Na_2SO_4. The solvent was evaporated to dryness to afford 0.11 g (99%) of a green−gray solid, **15**, mp 177 °C. ^{1}H NMR ($CDCl_3$, 300 MHz): δ 7.82 (d, J = 6.00 Hz, 1H), 7.42 (s, 1H), 7.30 (t, J = 5.70 Hz, 1H), 7.27 (t, J = 6.00 Hz, 1H), 7.06 (t, J = 6.00 Hz, 1H), 6.86 (s, 1H), 3.72 (s, 3H), 1.25 (s, 9H). ^{13}C NMR: δ 144.1, 140.5, 130.0, 128.7, 122.6, 122.2, 117.0, 116.8, 115.2, 108.1, 106.4, 33.1, 28.9, 27.9. IR (cm^{-1}): ν 3241. HRMS (FAB+): calcd for $C_{17}H_{19}NO_2$, 269.1416; found, 269.1398.

9*N*-Methyl-4-*t*-butylcarbazole orthoquinone (16). Using the general method described in the Supporting Information, this

compound was obtained in 97% yield as a green solid (CH_2Cl_2), **16**, mp 162−164 °C. ^{1}H NMR ($CDCl_3$, 300 MHz): δ 7.69 (dd, J = 8.1, 1.2 Hz, 1H), 7.43 (t, J = 7.8 Hz, 1H), 7.41 (d, J = 7.5 Hz, 1H), 7.36 (s, 1H), 7.34 (dt, J = 9.0, 0.9 Hz, 1H), 7.23 (dt, J = 7.8, 0.9 Hz, 1H), 4.05 (s, 3H), 1.31 (s, 9H). ^{13}C NMR: δ 198.7, 182.1, 147.7, 140.4, 130.5, 128.4, 122.8, 121.0, 115.8, 114.2, 111.3, 101.4, 54.1, 35.1, 29.8. IR (cm^{-1}): ν 1659. HRMS (M + H) (FAB+): calcd for $C_{17}H_{19}NO_2$, 268.1338; found, 268.1335.

9*N*-Methyl-4-*t*-butylcarbazole semiquinone (17). Using the general procedure described in the Supporting Information, this compound was generated in situ, and EPR measurements were conducted. Electrochemical preparation of **17** was accomplished by placing **16** (0.00141 g, 0.0053 mmol) and electrolyte *n*-Bu_4NPF_6 (0.21 g, 0.55 mmol) in 5.5 mL of anhydrous THF. Cyclic voltammetric measurements were then conducted on the solution, with Pt wire serving as the working and auxiliary electrodes, while the reference electrode was $Ag/AgNO_3$ in acetonitrile.

1-Hydroxydibenzofuran (19). To a 200 mL Schlenk flask equipped with a stir bar and nitrogen adapter were added dibenzofuran-1-boronic acid, **18** (1.0 g, 4.72 mmol), 30% hydrogen peroxide (11.13 mL, 23.58 mmol), 2% sodium hydroxide solution (18.0 mL), and 30 mL of dry THF. The resulting suspension was stirred at room temperature for 24 h under nitrogen. The solvent was removed under reduced pressure, and the residue was taken up in diethyl ether, acidified with 2% HCl solution (20 mL), separated, and the aqueous layer extracted with diethyl ether. The organic portions were combined and evaporated to dryness to afford 0.82 g (94%) of a pale yellow solid, **19**, mp 102−104 °C. ^{1}H NMR: δ 7.94 (dd, J = 1.5, 7.5 Hz, 1H), 7.58 (d, J = 8.4 Hz, 1H), 7.53 (dd, J = 1.0, 7.8 Hz, 1H), 7.47 (dt, J = 0.8, 7.8 Hz, 1H), 7.36 (dt, J = 1.2, 6.3 Hz, 1H), 7.23 (t, J = 7.5 Hz, 1H), 7.09 (dd, J = 1.2, 7.9 Hz, 1H), 5.31 (s, 1H). ^{13}C NMR: δ 156.2, 145.6, 127.9, 126.5, 124.0, 123.5, 122.2, 113.5, 112.2, 111.4, 110.4, 109.5. HRMS (EI+): calcd for $C_{22}H_8O_2$, 184.0524; found, 184.0530.

1-Methoxydibenzofuran (20). To a 100 mL round-bottom flask equipped with a stir bar were added **19** (0.79 g, 4.29 mmol), potassium carbonate (1.19 g, 8.58 mmol), 18-crown-6 (10 mol %), and 50 mL of acetone, and the mixture was stirred for 15 min. Then, methyl iodide (0.80 mL, 12.87 mmol) was added dropwise, a reflux condenser added, and the mixture refluxed for 24 h under nitrogen. The solvent was removed under reduced pressure, and the residue was taken up in methylene chloride, acidified with 2% HCl solution (20 mL), separated, and the aqueous layer again extracted with methylene chloride. The organic portions were combined, filtered through a silica gel plug, and evaporated to dryness to afford 0.78 g (91%) of a pale yellow solid, **20**, mp 52−54 °C. ^{1}H NMR: δ 7.94 (d, J = 7.7 Hz, 1H), 7.63 (d, J = 8.2 Hz, 1H), 7.56 (d, J = 7.8 Hz, 1H), 7.47 (dt, J = 1.2, 7.5 Hz, 1H), 7.35 (dt, J = 0.8, 7.4 Hz, 1H), 7.29 (t, J = 7.7 Hz, 1H), 7.01 (d, J = 8.1 Hz, 1H), 4.08 (s, 3H). ^{13}C NMR: δ 156.2, 145.6, 127.9, 126.5, 124.0, 123.5, 122.2, 113.5, 112.2, 111.4, 110.4, 109, 56.8. HRMS (EI+): calcd for $C_{23}H_{10}O_2$, 198.0681; found, 198.0672.

2-Hydroxy-1-methoxydibenzofuran (21). To a 200 mL Schlenk flask equipped with a stir bar and nitrogen adapter were added **20** (2.93 g, 14.8mmol) and 70 mL of dry THF, and the solution was cooled to −78 °C under N_2. Then, *t*-BuLi (19.1 mL, 32.5 mmol) was added dropwise slowly with stirring. After 2 h, trimethyl borate (5.04 mL, 44.4 mmol) was added dropwise and allowed to warm to room temperature overnight. The solvent and excess trimethyl borate were removed under reduced pressure, and 70 mL of dry THF, 30% hydrogen peroxide (11.71 mL, 23.58 mmol), and 2% sodium hydroxide solution (18.0 mL) were added. The resulting suspension was stirred at room temperature for 24 h under nitrogen. The solvent was removed under reduced pressure, the residue taken up in diethyl ether, acidified with 2% HCl solution (20 mL), separated, and the aqueous layer extracted with diethyl ether. The organic portions were combined and evaporated to dryness to afford 2.82 g (89%) of a tan solid, **21**, mp 84−88 °C. ^{1}H NMR: δ 7.85 (d, J = 7.5 Hz), 7.54 (d, J = 8.0 Hz), 7.49 (d, J = 8.3 Hz, 1H), 7.38 (t, J = 7.5 Hz, 2H), 7.31 (t, J = 7.3 Hz, 2H), 6.97 (d, J = 8.3 Hz, 1H), 4.29 (s, 3H). ^{13}C NMR: δ 156.6, 147.7, 147.3, 132.3, 126.1, 124.7, 123.1, 120.9, 119.2, 114.7, 111.7, 111.6, 61.2. HRMS (EI+): calcd for $C_{13}H_{10}O_3$, 214.0630; found, 214.0625.

1,2-Dimethoxydibenzofuran (22). To a 100 mL round-bottom flask equipped with a stir bar were added **21** (0.71 g, 3.33 mmol), potassium carbonate (0.92 g, 6.66 mmol), 18-crown-6 (10 mol %), and 50 mL of acetone, and the mixture was stirred for 15 min. Then, methyl iodide (0.31 mL, 5.0 mmol) was added dropwise, and the mixture was refluxed under nitrogen. After 6 h, another aliquot of methyl iodide (0.31 mL, 5.0 mmol) was added and the mixture refluxed for 42 h. The solvent was removed under reduced pressure, the residue taken up in methylene chloride, acidified with 1 M HCl solution (20 mL), separated, and the aqueous layer again extracted with methylene chloride. The organic portions were combined, filtered through a silica gel plug, and evaporated to dryness to afford 0.76 g (99%) of a pale yellow solid, **22**, mp 102−104 °C. ^{1}H NMR: δ 7.86 (dd, J = 8.7, 1.0 Hz, 1H), 7.55 (dd, J = 8.1, 1.8 Hz, 2H), 7.40 (dt, J = 7.4, 1.5 Hz, 1H), 7.31 (dt, J = 7.35, 0.9 Hz, 1H), 6.96 (d, J = 8.7 Hz, 1H), 4.21 (s, 3H), 3.97 (s, 3H). ^{13}C NMR: δ 156.7, 151.5, 147.7, 136.3, 126.5, 124.6, 123.1, 120.3, 120.0, 114.4, 111.8, 108.7, 61.5, 57.2. HRMS (EI+): calcd for $C_{13}H_{10}O_3$, 228.0786; found, 228.0785.

3-*t*-Butyl-1,2-dimethoxydibenzofuran (23a) and 8-*t*-Butyl-1,2-dimethoxydibenzofuran (23b). To a 50 mL round-bottom flask equipped with a stir bar, condenser, and septum were added **22** (0.75 g, 2.33 mmol), H_3PO_4 (0.81 g, 5.85 mmol), and PPA (1.87 g). The reaction mixture was heated to 76 °C under nitrogen and stirred for 15 min. Then, *t*-butanol (0.20 mL, 3.04 mmol) was added to the reaction mixture, and after 1 h, another 0.20 mL aliquot of *t*-butanol was added. The reaction was allowed to proceed for 24 h. The oily residue was washed with 20% NaOH solution (20 mL), extracted with CH_2Cl_2, separated, the organic layer dried over Na_2SO_4 and subjected to radial chromatography (0−50% ether/pet ether) to afford 0.20 g (21%) of colorless crystals, **23a**, mp 90−93 °C, and 0.17 g (17%) of a brownish oil, **23b**, as a second fraction. **23a:** ^{1}H NMR: δ 7.85 (dd, J = 0.6, 7.2 Hz, 1H), 7.56 (d, J = 8.4 Hz, 1H), 7.46 (d, J = 0.9 Hz, 1H), 7.45 (d, J = 2.1 Hz, 1H), 6.95 (d, J = 8.7 Hz, 1H), 4.19 (s, 3H), 3.97 (s, 3H), 1.42 (s, 9H). ^{13}C NMR: δ 152.1, 150.0, 151.3, 148.3, 133.6, 130.4, 128.7, 122.9, 121.0, 117.8, 114.2, 113.0, 112.3, 56.4, 56.1, 34.8, 31.6. HRMS (EI+): calcd for $C_{13}H_{10}O_3$, 284.1412; found, 284.1403. **23b:** ^{1}H NMR: δ 7.78 (dd, J = 0.6, 7.1 Hz, 1H), 7.22 (dd, J = 0.6, 7.2 Hz, 1H), 7.05 (m, 1H), 6.91 (m, 2H), 4.09 (s, 3H), 3.89 (s, 3H), 1.34 (s, 9H). ^{13}C NMR: δ 156.4, 154.9, 151.3, 146.2, 124.2, 120.6, 116.7, 114.2, 111.1, 108.5, 106.0, 104.9, 61.4, 57.3, 35.0, 32.1. HRMS (EI+): calcd for $C_{13}H_{10}O_3$, 284.1412; found, 284.1419.

3-*t*-Butyl-1,2-dihydroxydibenzofuran (24a). Using method B described in the Supporting Information, this compound was obtained in 94% yield as colorless crystals, mp 61−64 °C. ^{1}H NMR: δ 7.85 (s, 1H), 7.44 (s, 2H), 7.38 (d, J = 7.9 Hz, 1H), 6.93 (d, J = 8.1 Hz, 1H), 5.50 (br s, 2H), 1.41 (s, 9H). ^{13}C NMR: δ 154.9, 146.4, 143.6, 128.9, 123.9, 116.9, 112.3, 111.6, 110.9, 35.1, 32.1. IR (cm^{-1}): ν 3170. HRMS (EI+): calcd for $C_{16}H_{16}O_3$, 256.1099; found, 256.1099.

8-*t*-Butyl-1,2-dihydroxydibenzofuran (24b). Using method B described in the Supporting Information, this compound was obtained in 94% yield as a brown oil. ^{1}H NMR: δ 7.71 (d, J = 8.1 Hz, 1H), 7.48 (s, 1H), 7.38 (m, 2H), 6.96 (t, J = 7.2 Hz, 1H), 6.10 (br s, 2H), 1.38 (s, 9H). ^{13}C NMR: δ 143.5, 129.1, 123.9, 123.1, 120.8, 119.7, 119.1, 118.3, 116.8, 112.1, 111.6, 108.6, 35.4, 31.9. IR (cm^{-1}): ν 3365. HRMS (EI+): calcd for $C_{16}H_{16}O_3$, 256.1099; found, 256.1100.

3-*t*-Butyldibenzofuran semiquinone (25a). Using the procedure described for compound **10**, this compound was generated in situ (0.5 mM in THF), and EPR measurements were conducted.

8-*t*-Butyldibenzofuran semiquinone (25b). Using the procedure

described for compound **10**, this compound was generated in situ (0.5 mM in THF), and EPR measurements were conducted.

Acknowledgment. The authors would like to thank the USMA Center for Molecular Science for computational support, and the NCSU Mass Spectroscopy Facility for high-resolution MS analysis. D.A.S. thanks the NSF (CHE-0345263) for support of this work.

Supporting Information Available: General experimental methods, ^{1}H or ^{13}C NMR spectra, cyclic voltammograms, and density functional theory computational parameters for reported compounds. This material is available free of charge via the Internet at http://pubs.acs.org.

JO061502J